Molecular Crystals and Liquid Crystals
Publication details, including instructions for authors and subscription information:
http://www.tandfonline.com/loi/gmcl16

The Electronic Structure of the Furan-quinones

C. H. Griffiths [a] , M. S. Walker [a] , P. Goldstein [a] & R. L. Miller [a]
[a] Xerox Corporation, Webster Research Center, Webster, New York, 14580

Version of record first published: 29 Aug 2007.

To cite this article: C. H. Griffiths , M. S. Walker , P. Goldstein & R. L. Miller (1975): The Electronic Structure of the Furan-quinones, Molecular Crystals and Liquid Crystals, 31:3-4, 295-304

To link to this article: http://dx.doi.org/10.1080/15421407508082882

Mol. Cryst. Liq. Cryst., 1975, Vol. 31, pp. 295–304

Printed in Holland

The Electronic Structure of the Furan-quinones

Polymorphism in Dinaphtho[1,2-2′,3′]furan-7,12-dione

C. H. GRIFFITHS, M. S. WALKER, P. GOLDSTEIN and R. L. MILLER
Xerox Corporation, Webster Research Center, Webster, New York 14580

(*Received July 11, 1975*)

Two polymorphic modifications, a stable orange monoclinic form (mp 231°C) and a metastable yellow orthorhomic form (mp 228.5°C) of dinaphtho[1,2-2′,3′]furan-7,12-dione have been indentified by single crystal X-ray diffraction. The transition from the metastable to the stable phase occurred rapidly at melting and slowly just below the melting temperature.

Fluorescence and long wavelength absorption spectra indicate greater overlap of adjacent molecules in the monoclinic phase and this is supported by the greater calculated X-ray density. Differences in molecular packing between this furan-quinone and the isomeric dinaphtho-[2,1-2′,3′]furan-8,13-dione are probably due to a significant departure from planarity in the former caused by the proximity of the quinone oxygen and the benzene ring.

INTRODUCTION

Many organic and inorganic materials form more than one kind of crystal having different physical and thermodynamic properties. As early as 1942 Deffet[1] listed nearly 1200 organic materials in which polymorphism had been detected and more recently Warwicker[2] has shown that polymorphism is a common phenomenon in anthraquinone vat dyes. While a change in optical absorption in the visible region of the spectrum is not a necessary result of the crystallographic differences in polymorphs, such a change in observable color does often occur.

The furan-quinones have been shown to be suitable as vat dyes[3] and polymorphism in dinaphtho[2,1-2′,3′]furan-8,13-dione has been discussed in detail by Walker *et al.*[4] In this work two yellow phases (α and β) and an orange phase (γ) are described having respectively 4,4 and 2 molecules per unit cell. The system is apparently monotropic and the β and γ phases transform exothermically to the α phase. Here we have characterized the polymorphs of the isomeric dinaphtho[1,2-2′,3′]furan-7,12-dione using calorimetric, structural and spectroscopic techniques and compared them to the previously discussed polymorphs of the structural isomer. The molecular structure of the two isomeric furan-quinones is shown in Figure 1.

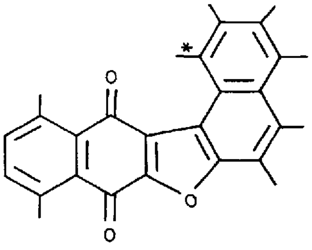

I

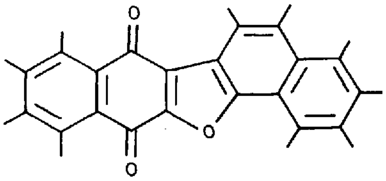

II

FIGURE 1 Molecular structure of dinaphtho[2,1-2′,3′]furan-8,13-dione (I) and dinaphtho-[1,2-2′,3′]furan-7,12-dione (II).

EXPERIMENTAL

The dinaphtho[1,2-2′,3′]furan-7,12-dione (furan-quinone II) was synthesized by refluxing 2,3-dichloro-1,4-naphthoquinone with α-naphthol in anhydrous pyridine.[5,6] The material was then recrystallized from methanol several times and vacuum sublimed. Microanalysis gave H, 3.60% and C, 80.64% whereas the molecular formula $C_2H_{10}O_3$ requires H, 3.40% and C, 80.5%.

Crystals were grown in a quartz tube in a temperature gradient furnace using flowing nitrogen as a transport gas. Sublimation from a quartz boat in air onto a heated quartz substrate with a gradient from approximately 200 to 230°C produced similar needle shaped crystals. Crystals were also grown from solution by slow cooling of saturated solutions in benzene, chloroform, methanol and acetone. X-ray patterns were recorded on precession and Weissenberg cameras with CuK_α radiation. Polaroid high speed film was employed in the precession camera and Kodak or Ilford X-ray film in the Weissenberg camera. Measurements on precession photographs enabled lattice parameters to be determined to an estimated accuracy of 0.3% of the distance and 0.1% in the angles. Crystals ranging in thickness from 0.03 to 0.1 mm were used for these measurements.

Calorimetry was carried out using a Dupont Model 900 Differential Thermal Analyzer with a Differential Scanning Calorimeter (DSC) attachment. The temperature scale and calorimetric measurements were calibrated at the temperature ranges of interest directly against known melting points and heats of fusion. Weighed samples were sealed in aluminum pans and areas under the transition peaks in the thermograms were measured with a K and E compensating polar planimeter.

Ultra-violet and visible absorption and emission spectra were recorded on a Cary 14 Recording Spectrophotometer and an Aminco-Kiers Spectrophotofluorimeter respectively. All spectra were recorded at ambient temperature.

RESULTS

A Morphology and Crystal Structure

The furan-quinone II was obtained in two obviously different forms from both the vapour phase and solution. After sublimation onto the heated substrate the crystals were needle shaped with an approximately square cross section. Those crystals in the high end of the substrate temperature gradient were orange in colour and those in the low end of the gradient were yellow. The division between the two phases occurred at approximately 210°C but this dividing line was not sharp.

Crystals grown by slow cooling from polar solvents such as methanol and acetone in which the furan-quinone II had a relatively high solubility were of the orange variety. Those grown by slow cooling from relatively non-polar solvents such as benzene and chloroform in which the material was much less soluble were of the yellow phase. More rapid cooling of the solutions in acetone and methanol again produced the yellow phase. These crystals were similar in properties to those grown from the vapour phase but were of much smaller dimensions.

Samples of the vapour grown crystals were selected for X-ray diffraction analysis and studied in detail. The two phases of the material, yellow and orange, were found to correspond to two crystallographically distinct structures. Table I gives the unit cell data for these two structures. The Okl and hOl zone diffraction patterns of the two phases were very similar, indicating very similar packing arrangements when viewed down the a or b axes of the unit cell. The two hkO zones were however quite different.

TABLE I

Lattice Parameters and Space Group Data for Polymorphs of Dinaphtho[1,2-2′,3′]Furan-7,12-Dione

	a(Å)	b(Å)	c(Å)	β(deg)	V(Å^3)	ρ(g/cc)	N	Sp. Gp.
yellow (orthorhombic)	27.2_0	3.69_0	13.7_3	90	1378	1.438	4	$Pna2_1$
orange (monoclinic)	27.4_1	3.67_1	27.3_1	92.5	2744	1.444	8	$P2_1/n$ or $P2_1/c$

* a, b, c are the unit cell dimensions; β is the monoclinic angle, V the volume of the unit cell and ρ the density deduced from the x-ray data; N is the number of monomeric units per unit cell and Sp. Gp. is the most probable space group.

In both the yellow and the orange phases the b axis was parallel to the long axis of the needle and in the yellow phase the faces of the needle were of the {201} type shown in Figure 2. The crystals of the orange polymorph appeared similar to those of the yellow polymorph but were actually twinned. This twinning, described by a 180° rotation about the "a" axis shown in Figure 3, imparts a higher symmetry to the diffraction pattern. The superposition of the twins apparently leads to a composite crystal having an external appearance similar to the yellow phase. The same type of twinning has been observed previously in Para-Red (*p*-nitrophenylazo-2-naphthol).[7]

The monoclinic unit cell of the orange polymorph closely resembles the orthorhombic unit cell of the yellow polymorph except for the doubling in length of the c-axis. The systematic absences, hOl:h = 2n and Okl:K + l = 2n imply a space group $Pna2_1$ for the yellow phase. For the orange phase the systematic absences hOl:h + l = 2n and OkO:K = 2n limit the space

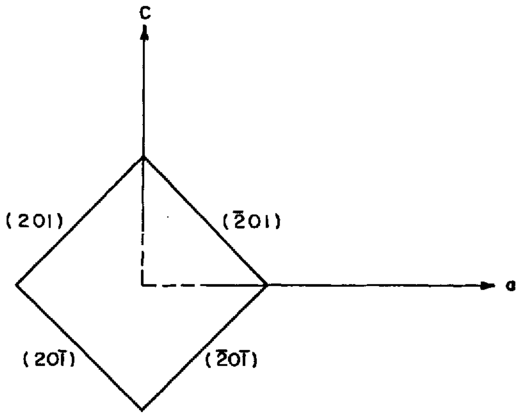

FIGURE 2 Schematic cross-section of a needle crystal of the yellow orthorhombic phase of dinaphtho[1,2-2′,3′]furan-7,12-dione.

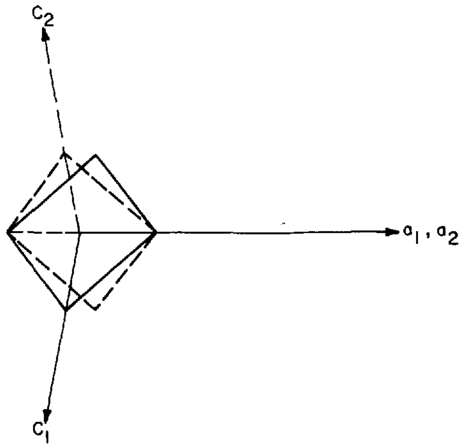

FIGURE 3 Schematic cross-section of a crystal of the orange monoclinic phase of dinaphtho-[1,2-2′,3′]furan-7,12-dione.

groups to $P2_1/n_1$ $P2_1/c$ or $P2_1/a$ and $P2_1/a$ can be eliminated on molecular symmetry grounds.

B Calorimetric Measurements

Samples of the yellow and orange phases of dinaphtho[1,2-2′,3′]furan-7,12-dione were run in the DSC cell at heating rates from 1 to 30°C/minute. At the higher heating rates (> 20°/minute) the yellow phase gave a thermogram with no indication of any change of state below the melting point at 228.5°C. The orange phase gave a similarly uneventful thermogram but melted 2.5°C higher at 231°C. At lower heating rates the orange phase maintained the single melting endotherm with an extrapolated onset at 231°C. Significant changes were, however, observed in the thermogram from the yellow phase. The single melting endotherm was resolved into a double endotherm indicating a second melting point with an extrapolated onset at 231°C. This second melting point is the same as that obtained with samples of the orange phase. At 5°C/minute the amplitude of the 231° endotherm was only 30 % of that of the 228.5° endotherm. The relative size of the 231°C endotherm increased with decreasing heating rate. At 2.5°C/minute the two amplitudes were equal and at 1°C/minute the 228.5°C endotherm was only 28 % of the 231°C endotherm. The thermograms obtained by heating at 1°C/minute and 5°C/minute are shown in Figure 4. It should be noted that at the slower heating rate an obvious exotherm occurs between the two melting endotherms.

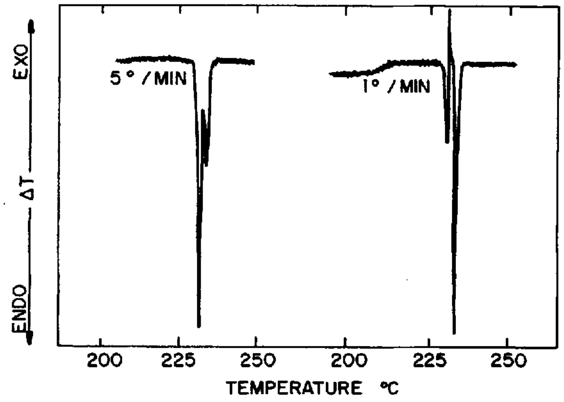

FIGURE 4 Thermograms from the yellow orthorhombic phase of dinaphtho[1,2-2′,3′]furan-7,12-dione.

There was no change in structure of the thermograms below the yellow phase melting point with decreasing heating rate other than a small change in baseline beginning at about 212°C when scanning this phase. Samples of the yellow phase heated at 1°/minute and quenched at a few degrees below the melting point showed some conversion to isolated needle crystals of the orange phase. When quenched between the first and second melting endotherms there was complete recrystallization to large crystals of the orange phase. Quenching after the second endotherm gave a solid crystalline orange mass. Samples heated isothermally at 221°C for 30 minutes showed complete conversion to the orange phase, however the size and shape of the needle crystals indicated conversion via the vapour phase.

C Visible Absorption and Emission Spectra

No single crystal absorption spectra could be recorded for the two polymorphs due to the lack of suitable crystals. Absorption spectra were, however, recorded for the yellow polymorph dispersed in a potassium bromide matrix and for a thin film of the furan-quinone vacuum deposited onto a quartz slide (Figure 5). The latter spectrum may be compared to the molecular absorption spectrum of the quinone dissolved in hexane also shown on Figure 5. It was not possible to obtain a reproducible absorption spectrum of the orange form in KBr due to some instability of this polymorph during sample preparation. Absorption spectra were, however, recorded for both polymorphs dispersed in nujol mulls.

The long wavelength absorption band of the yellow form exhibits a peak at 440 nm ($\alpha \sim 8 \times 10^4$ cm^{-1}) with shoulders at approximately 415 nm

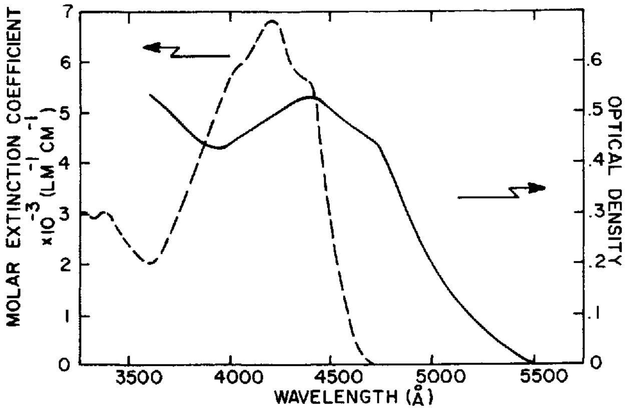

FIGURE 5 Absorption spectra of dinaphtho[1,2-2′,3′]furan-7,12-dione (a) as a thin film on quartz (continuous line) and (b) dissolved in hexane (dashed line).

and 465 nm. Other absorption bands are located at 345 nm, 295 nm and 265 nm. The long wavelength band of the orange form shows a peak near 435 nm with a shoulder near 465 nm. The wavelengths for the latter polymorph are taken from the mull spectra which were not well resolved due to scattering effects. Whilst the peak wavelengths for the analogous absorption bands in the two forms are similar, the absorption bandwidth for the orange form is the greater. This results in a shift in the absorption edge to longer wavelengths for the latter which gives rise to its orange color.

The frequency separation between the components is approximately 1200 cm^{-1} in both spectra. This frequency, which corresponds closely to the vibrational spacing of ~1100 cm^{-1} observed in the analogous molecular transition, is tentatively associated with the furan C—O—C stretching vibration.

Fluorescence emission spectra were recorded to further characterize these polymorphs. Single crystals were mounted on quartz slides and excited with 350 nm radiation and the emission viewed normal to the front surface of the crystals. No vibrational structure was noted in the spectra and peaks were located at 580 and 600 nm (uncorrected) for the yellow and orange forms respectively.

The spectra did not exhibit a mirror image relationship with the corresponding long wavelength absorption bands of the crystals and in fact were separated by some 350 cm^{-1} from the absorption peaks. These spectra may, however, be somewhat distorted by fluorescence reabsorption in the crystal (approximately 10 μ thick) which could account for the lack of mirror image symmetry.

DISCUSSION

X-ray analysis of vapour and solution grown crystals of dinaphtho[1,2-2′,3′]-furan-7,12-dione has indicated the existence of at least two polymorphs of this material. It is possible that polymorphs other than the yellow orthorhombic and orange monoclinic can be formed but no evidence for this possibility was uncovered in this study. The melting points and vapour phase transformations discussed above show that close to the melting point the orange monoclinic phase is the stable one. The exotherm seen at low heating rates following the melting endotherm of the yellow orthorhombic phase is apparently the recrystallization to the orange monoclinic phase. This is in turn closely followed by the melting endotherm of this latter phase. The recrystallization to the orange phase does not occur at higher heating rates due to a kinetic limitation. The transformation to the stable phase did occur below the melting point of the metastable phase. The visual appearance indicated both solid–solid and solid–vapour–solid reactions and the change in baseline of the 1°C/minute thermogram is probably due to the resultant, compaction of the material.

It was also observed that the orange phase was formed close to room temperature by slow cooling from solvents in which the material had an appreciable solubility whereas the yellow phase was produced when these solvents were cooled more rapidly and by slow cooling from less effective solvents.

It is known that the nucleation and growth of metastable phases is enhanced when conditions favour supersaturation.[8] Supersaturation occurs on rapid cooling and when the solubility and solute concentration are low. The formation of a nucleus of critical size requires the simultaneous collision of a critical number of monomer units. This critical size is reduced at temperatures below the saturation temperature and thus for kinetic reasons supersaturation occurs readily on cooling solutions in which the solute concentration is low. The formation of the orange phase by crystal growth under equilibrium conditions (high solubility, slow cooling) and the yellow phase under non-equilibrium conditions (low solubility, more rapid cooling) can be understood on the above basis. The orange phase is apparently the thermodynamically stable phase close to room temperature and the system is monotropic. The small increase in calculated density of the monoclinic orange phase structure over the orthorhombic yellow phase structure also supports this conclusion.

The furan-quinone II molecule is expected to be approximately planar and as such can be considered to be an ellipitical slab 3.6 Å thick. The 3.7 Å b-axis dimension in both polymorphs suggests that the plane of the molecules is close to normal to the axis and that the molecules form stacks which are parallel to the b-axis. In this case the small difference between the molecular dimension and the b axis spacing would be taken up by a slight tilt of the molecules with respect to the normal. The similarity in the Okl and hOl and lack of similarity in the hkO zone diffraction patterns indicates that the molecular packing is very similar in the yellow and orange polymorphs when viewed down the a and b-axes of the unit cell but dissimilar when viewed down the c-axis. In fact the periodicity of the unit cell is doubled in this direction in the orange phase with respect to the yellow phase.

The polymorphs of the furan-quinone II (Figure 1), their relative stabilities and molecular packing show very distinct differences from those previously described for the furan-quinone I.[4] An inspection of Figure 1 will show the proximity of the quinone oxygen in furan-quinone I to the hydrogen on the benzene ring carbon atom marked with an asterisk will probably produce a significant deviation from planarity for this molecule. This is evidenced by the lengths of the shortest axes in the three polymorphs of furan-quinone I. Only in the stable β-polymorph[4] does the b-axis (3.85 Å) approach the stacking axis period of the furan-quinone II polymorphs discussed above. The molecular packing in the α and γ polymorphs is not as obvious but is apparently not made up of simple stacks of molecules aligned parallel to the b-axis.

The similarity between the orthorhombic crystal and molecular long wavelength absorption spectra indicates a weak intermolecular interaction in this polymorph. The crystal shift in the long wavelength transition, as given by $\nu_{\text{hexane}} - \nu_{\text{crystal}}$, is approximately 1150 cm^{-1}. This shift is similar in magnitude to that observed for the α polymorph of the isomeric Dinaphtho-[2,1-2',3']furan-8,13-dione.[4]

The long wavelength absorption maximum for the orange monoclinic form also exhibits a shift relative to the molecular transition of about 1100 cm^{-1}. The increase in bandwidth, however, indicates the presence of a second transition at longer wavelengths. Unfortunately it was not possible to resolve out the maximum of this band due to the scattering component in the mull spectrum which prevented any meaningful de-convolution of the bands. The fluorescence spectra are, however, in agreement with this argument in that the emission from the monoclinic form is shifted some 600 cm^{-1} to lower energies of that from the yellow form.

The buried transition possibly results from increased intermolecular interaction due to a closer molecular spacing or greater overlap of adjacent molecules in the monoclinic structure. This is supported somewhat by the higher x-ray density calculated for the latter form. Shifts in the spectra of organic dyes have been attributed to dipole–dipole splitting of the molecular transition resulting from the formation of dimers, trimers and n-imers in the crystal lattice.[9] It is of interest to note that the quinone molecules in both polymorphs are stacked parallel to the b-axis with an intermolecular spacing of about 4 Å.

The molecular electron affinity and ionization potential of the furanquinone are 1.46 eV and 8.41 eV respectively.[10] Charge transfer interaction might, therefore, contribute to the stabilization of the lower electronic states of the monoclinic crystal. Complete crystal structures are required, however, for any further interpretation of the intermolecular interactions in these polymorphs.

References

1. L. Deffet, Répertoire des composés organiques polymorphes, Editions Desoer, Liege (1942).
2. J. O. Warwicker, *J. Text. Inst.* **50**, T443 (1959).
3. R. V. Ackarya, B. D. Tilak and M. R. Venkietswaran, *J. Sci. Ind. Res.*, **16B**, 400 (1957).
4. M. S. Walker, R. L. Miller, C. H. Griffiths and P. Goldstein, *Mol. Cryst. Liq. Cryst.* **16**, 203 (1972).
5. Ng. P. B. Hoi, *J. Chem. Soc.*, 489 (1952).
6. Ng. P. B. Hoi and P. Demerseman, *J. Chem. Soc.*, 4699 (1952).
7. C. T. Grainger and J. F. McConnell, *Acta Cryst.* **A25**, 422 (1969).
8. W. C. McCrone in Physics and Chemistry of the Organic Solid State, Vol. 2, Edited D. Fox, M. M. Labes and A. Weissberg, Interscience Publishers (1965).
9. E. S. Emerson, M. A. Conlin, A. E. Rosenoff, K. S. Norland, H. Rodriguez, D. Chin and G. L. Bird, *J. Phys. Chem.* **71**, 2396 (1967).
10. J. E. Kuder, D. Wychick, R. L. Miller and M. S. Walker, *J. Phys. Chem.*, **78**, 1714 (1974).